2013

The Importance of Spring and Autumn Atmospheric Conditions for the Evaporation Regime of Lake Superior

Christopher Spence
Environment Canada, Saskatoon, Saskatchewan, chris.spence@ec.gc.ca

P.D. Blanken
University of Colorado, Boulder

John D. Lenters
University of Nebraska-Lincoln, john.lenters@colorado.edu

N. Hedstrom
Environment Canada, Saskatoon

The Importance of Spring and Autumn Atmospheric Conditions for the Evaporation Regime of Lake Superior

C. SPENCE

Environment Canada, Saskatoon, Saskatchewan, Canada

P. D. BLANKEN

Department of Geography, University of Colorado Boulder, Boulder, Colorado

J. D. LENTERS

School of Natural Resources, University of Nebraska–Lincoln, Lincoln, Nebraska

N. HEDSTROM

Environment Canada, Saskatoon, Saskatchewan, Canada

(Manuscript received 26 November 2012, in final form 6 June 2013)

ABSTRACT

Feedbacks between ice extent and evaporation have long been suspected to be important for Lake Superior evaporation because it is during autumn and winter when latent heat fluxes are highest. Recent direct measurements of evaporation made at the Stannard Rock Lighthouse have provided new information on the physical controls on Lake Superior evaporation, in particular that evaporation can react within hours to days to a change in synoptic conditions. However, the large heat capacity of the lake creates a strong seasonal cycle of energy storage and release. There is a complex interaction among heat storage, evaporation, and ice cover that is highly dependent on atmospheric conditions in the spring and autumn ''shoulder seasons.'' Small changes in conditions in November and March caused by synoptic-scale events can have profound impacts on annual evaporation, the extent of ice cover, and the length of the ice-covered period. Early winter air temperatures in November and December dictate the nature of ice formation and much of the winter evaporative flux. Decreased ice cover, by itself, does not necessarily lead to enhanced annual evaporation losses. Rather, a combination of low ice cover and warm spring air temperatures, leading to an early breakup, can significantly lengthen the next evaporation season and cause greater cumulative water loss the subsequent year. The influence of individual synoptic events on annual evaporation is notable enough that the research community should ensure that their role is properly captured in numerical models to provide sound predictions of future Laurentian Great Lakes evaporation regimes.

1. Introduction

Until recently, Lake Superior surface energy budget and evaporation research has used model output (e.g., Derecki 1981; Beletsky et al. 1999), buoy-based meteorological measurements (e.g., Laird and Kristovich 2002), or remotely sensed data (e.g., Lofgren and Zhu 2000) to discern the physical controls of evaporation. It has been known for some time that there is a 5–6-month delay between peak energy input and latent heat release (Schertzer 1978; Lofgren and Zhu 2000). Studies have shown that monthly and seasonal evaporation exhibit a positive relationship with radiant heat transfer, air temperature, and cloud cover (Morton 1967; Croley and Assel 2002). Blanken et al. (2011) and Spence et al. (2011) describe direct measurements of evaporation that have recently provided new information on the physical controls on evaporation from Lake Superior. The evaporation response has a dichotomous relationship with conditions in the overlying atmosphere. While the large heat capacity of the lake is responsible for the lag between peak energy input and turbulent flux, Lake

Corresponding author address: Christopher Spence, Environment Canada, 11 Innovation Blvd., Saskatoon, SK S7N 3H5, Canada.
E-mail: chris.spence@ec.gc.ca

DOI: 10.1175/JHM-D-12-0170.1

Superior latent heat fluxes can be highly responsive to short-term changes in synoptic conditions (i.e., hours to days), specifically wind and vapor pressure, and particularly during unstable atmospheric conditions (Blanken et al. 2011). Evaporation over such a large water body is not spatially uniform, as evaporation rates vary with the movement of synoptic-scale air masses over the lake. While most evaporation occurs during relatively short-term events of 3 or 4 days, these episodes tend not to occur in isolated locations on the lake, but are spatially widespread. The exceptions to this rule are during periods of a stable atmosphere and low evaporation and when a transient ice cover can limit evaporation from some areas (Spence et al. 2011).

Evaporation accounts for 40% of losses from the lake, so changes in evaporation volumes can impact water levels (Neff and Nicholas 2005), particularly if these changes persist through time. Current Lake Superior water levels have been below normal since 1997, and 147-yr-old low-water marks were set in August and September 2007. Extreme lake levels on Lake Superior are largely driven by hydroclimatic factors (Stow et al. 2008) and can be cyclical. Previous low-water periods in the 1920s and early 1960s can be attributed to low precipitation and runoff into the lake. The current low-water period has been proposed to be anomalous, in that it is suspected to be associated primarily with increased lake evaporation (Assel et al. 2004; Hanrahan et al. 2010). Observed trends toward decreased ice cover extent and duration (Wang et al. 2012), stronger winds (Desai et al. 2009), and higher air and lake temperatures (Austin and Colman 2007) could lead to speculation that a stronger evaporation regime will be a new normal for Lake Superior.

Modeled evaporation rates, however, show that there was no increase in Lake Superior annual evaporation between 1948 and 1999 (Lenters 2004), despite being an indisputable period of higher mean annual air temperatures. Rather, the evaporation pattern displays an intriguing redistribution of the annual total from the winter months of November through February toward the summer and autumn months of July to October; a trend also noted by Hanrahan et al. (2010). Notwithstanding the nonlinear relationship between air temperature and evaporation via an exponential relationship between temperature and saturation vapor pressure, the results from Lenters (2004) and Hanrahan et al. (2010) imply that the relationship between air temperatures and Lake Superior evaporation is complex and relevant across a range of temporal scales.

It is often assumed that less ice on Lake Superior will result in higher annual evaporation (Wang et al. 2010), because it is during the autumn and winter months that evaporation rates are highest (Schertzer 1978; Lenters 2004; Blanken et al. 2011). However, the ice regime of Lake Superior and the other Laurentian Great Lakes is unlike that of other large northern lakes (e.g., Great Slave Lake) or smaller lakes at the same latitude (Mishra et al. 2011). Lake Superior rarely freezes completely, and the ice in any given location, especially offshore, is transient over time. This prevents complete cessation of winter evaporation and a reset of spring surface temperature following the annual breakup. The former phenomenon means that the lakewide fraction of ice cover may not be a good predictor of annual evaporation, particularly considering the amounts of evaporation that can occur in the presence of relatively high fractional ice cover (e.g., Gerbush et al. 2008). The implication is increased persistence in the lake temperature regime. At least a moderately long observational record is needed to explain how annual evaporation from such a large lake responds to atmospheric conditions. Data from the field campaign introduced by Blanken et al. (2011) have now been collected for four years, across a variety of meteorological conditions and within the range of near-record maximum and minimum ice cover. This allows for the investigation of the physical processes that control how Lake Superior evaporation rates vary over time scales of several months to years, which is the focus of this study. In particular, aspects of the relationship between ice and evaporation regimes of Lake Superior are discussed.

2. Methods

Stannard Rock Light (47.183°N, 87.225°W) provides an excellent, year-round offshore platform for meteorological observations, as well as good exposure for turbulent flux measurements, given its location 39 km from the nearest shore and 32 m above the water (Fig. 1). The results of Spence et al. (2011) imply that while there can be significant differences between evaporation rates observed at Stannard Rock Light and those estimated across the entire lake for short periods because of variation in surface water temperatures and atmospheric conditions, measurements of annual evaporation are typically within 10% of those from the entire lake. Stannard Rock Light is National Oceanic and Atmospheric Administration (NOAA) National Data Buoy Center (NDBC) station STDM4, providing meteorological data since 1984.

An enhanced observation program that includes eddy covariance and supporting meteorological instruments began on 1 June 2008 to the present (June 2013) to directly measure evaporation and associated meteorological conditions. The period for this study was from 1 June 2008 to 2 April 2012. Turbulent fluxes of sensible and latent heat (H and λE, respectively; W m^{-2} positive upward from the

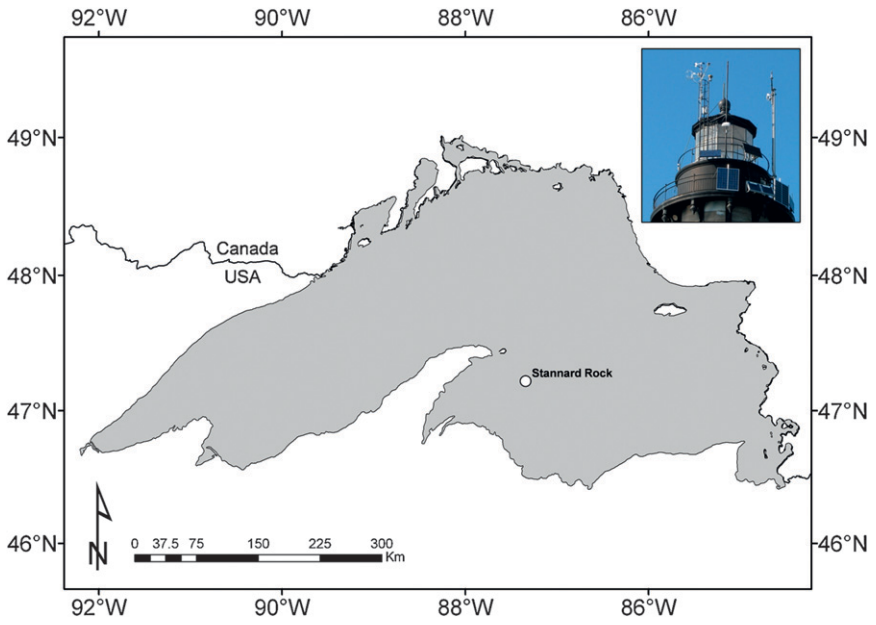

FIG. 1. Lake Superior, showing the location of Stannard Rock Light, and an inset photo of meteorological instrumentation.

surface) were calculated from 10-Hz measurements of the vertical wind speed (w; $\mathrm{m\,s^{-1}}$), air temperature (T; °C), and water vapor density (q; $\mathrm{g\,m^{-3}}$). Wind speed was measured using a 3D ultrasonic anemometer (Campbell Scientific CSAT-3), while water vapor density was measured using an open path gas analyzer (LI-COR 7500A open path CO_2/H_2O gas analyzer) located 15 cm away and at the same height as the sonic anemometer. The statistics (means and covariances) of the high-frequency data were collected and processed at 30-min intervals using a datalogger (Campbell Scientific CR3000). Corrections to the eddy covariance measurements included 2D coordinate rotation (Baldocchi et al. 1988), and corrections for air density fluctuations (Webb et al. 1980), sonic pathlength, high-frequency attenuation, and sensor separation (Massman 2000; Horst 1997).

There were short periods, hours in length, during each summer when poor quality data were produced. It is suspected this was when the boundary layer was too shallow to reach the 32-m height of the sensors. Data during these periods were filtered out and not used in calculations of daily latent heat flux λE and evaporation E. The only extended period with a gap in observed data occurred from 20 March to 10 May 2009 because of power failure. Evaporation during this period was estimated from an empirical equation based on wind speed and vapor pressure derived by Blanken et al. (2011). Input data were obtained from the NOAA Great Lakes Environmental Laboratory operational evaporation model because the NOAA station STDM4 was also inoperable at this time. The measurement footprint, defined as the upwind distance within which 90% of the turbulent fluxes originate, was calculated using the solutions of Schuepp et al. (1990), with corrections added for atmospheric stability based on the 24-h median value of the Obukhov stability length. This footprint was calculated to be 12.5 ± 2.5 km upwind of Stannard Rock Light during the range of atmospheric stability conditions observed during the study period. Using a footprint-based radius to designate the source area was deemed acceptable since the surface is the same in all directions.

On the same mast, slow 5-s samples of ancillary meteorological variables were also measured, with 30-min statistics collected on the same datalogger as the high-frequency data. Air temperature at 32-m elevation (T_{32}; °C) and vapor pressure (e_{32}; kPa) were measured with a shielded thermohygrometer (Vaisala HMP45C). Water surface temperature (T_0; °C) was measured with an infrared thermometer (Apogee IRR-T), from which surface saturation vapor pressure was calculated (e_0; kPa).

Biweekly ice cover data across the lake and within the turbulent flux footprint were obtained from the Canadian Ice Service (www.ice.ec.gc.ca). Output from the Great Lakes Surface Environmental Analysis (GLSEA) was used to define longer-term (1994–2010) Lake Superior surface water temperature regimes. These data (from http://coastwatch.glerl.noaa.gov) were obtained from the NOAA polar orbiting satellite-mounted Advanced Very High Resolution Radiometer (AVHRR). Lake surface temperatures are updated daily using information from

the cloud-free portions of the previous day's satellite imagery. If no imagery is available, a smoothing algorithm is applied to the previous day's estimate.

Incident shortwave ($S^{\downarrow}$; W m^{-2}) and longwave radiation ($L^{\downarrow}$; W m^{-2}) were measured with radiometers. Net radiation (Q^*; W m^{-2}) was calculated from

$$Q^* = S^{\downarrow}(1 - \alpha) + L^{\downarrow} - L^{\uparrow} \quad (1)$$

using measured $S^{\downarrow}$ and $L^{\downarrow}$, with ice-free and ice shortwave albedo (α) set to 0.08 and 0.8, respectively, based on direct measurements made over adjacent Lake Huron. Total outgoing longwave radiation ($L^{\uparrow}$; W m^{-2})—the sum of emitted and reflected—was calculated using measured infrared water surface temperature (T_0; K), the Stefan–Boltzmann Law (where σ is the Stefan–Boltzmann constant), and an assumed emissivity (ε) of 0.98 (i.e., reflected longwave was set equal to 2% of $L^{\downarrow}$). Because of logistical constraints of operating buoys through the winter season on Lake Superior, direct measurements of the rate of heat storage in the lake (J_w; W m^{-2}) within the vicinity of the flux footprint were not performed as part of this study but were estimated as a residual of the energy balance

$$J_w = Q^* - \lambda E - H. \quad (2)$$

The error in eddy covariance–based turbulent fluxes is commonly quantified based on the degree of energy budget closure. Blanken et al. (2011) showed that the Lake Superior heat storage term, estimated as a residual of the energy balance, compared well with those calculated by Schertzer (1978) using measured water temperature profiles. This provides confidence that the estimates of λE and H are likely within the 10%–20% of the actual values within the turbulent flux footprint, documented in other studies applying the eddy covariance method over water (Tanny et al. 2007). Lake heat storage (MJ m^{-2}) and cumulative evaporation (millimeters) were calculated for each evaporation year. The beginning of the evaporation year was defined as the end of the final week during which the Canadian Ice Service documented ice on the lake (i.e., the ice-free date). This was assumed to be the point in time after which subsequent energy added to the lake would drive evaporation within the next ~365 days.

3. Results

a. Evaporation year 2008/09

The beginning of the observation period (June 2008) began under stable atmospheric conditions, low evaporation rates, and high energy input into the lake (Figs. 2, 3; Tables 1, 2). The vapor pressure gradient became positive on 5 August 2008, at which time evaporation rates steadily increased through December 2008. Frequent passage of cold air masses in November 2008 resulted in a below-average air temperature (T_{32} = 2.2°C) and a high number of freezing degree-days (FDD = 29). This led to a loss of 404 MJ m^{-2} of heat from the lake that month (Fig. 3) through strong turbulent fluxes, with a low Bowen ratio of 0.32 indicating that evaporative cooling was roughly 3 times greater than sensible heat fluxes early in the winter. The large heat loss resulted in the onset of ice formation two weeks earlier than the median date. It was not until roughly half of the flux footprint was covered by ice (on 27 January 2009) that evaporation rates were significantly reduced (Figs. 2, 4). March 2009 air temperatures were below average (T_{32} = −3.2°C) with an extensive ice cover present across the footprint, as well as the entire lake (Table 1). Cumulative evaporation for 2008/09 was estimated to be 520 mm. The length of the evaporation year was 358 days, for an average evaporation rate of 1.5 mm day^{-1} (Table 2, Fig. 4).

b. Evaporation year 2009/10

The 2009/10 evaporation year began with cool spring conditions and a low T_0 on 1 June of 2.7°C (Table 1). As in the summer of 2008, early season evaporation was suppressed by negative vapor pressure gradients (Fig. 2), and almost all summer net radiation was directed to heat storage (Table 1). November 2009 was warmer, with only one FDD and a T_{32} that was 3.3°C higher than the previous year. With November temperature and vapor pressure gradients generally negative, only 107 MJ m^{-2} of heat was lost (Fig. 3). This reflects significantly lower evaporation rates during November 2009, roughly half those of November 2008. As such, the lake did not lose enough heat early in the winter to permit offshore locations within the flux footprint to freeze. This allowed evaporation rates to remain steady through late winter, but higher air temperatures (perhaps due in part to the lack of ice) resulted in a switch toward negative temperature gradients, lower vapor pressure gradients, and a suppression of evaporation in March 2010 (Fig. 2). Thus, average evaporation rates in March 2009 and 2010 were almost equal, despite the vastly different ice cover fractions within the tower footprint. Furthermore, evaporation totals and daily average rates for the 2009/10 evaporation year (525 mm, 1.6 mm day^{-1}) were nearly equal to those in 2008/09 (520 mm, 1.5 mm day^{-1}; Table 2, Fig. 4).

c. Evaporation year 2010/11

Positive Q^* by 9 February 2010 (Fig. 3, Table 1), in combination with mild air temperatures and a low ice cover in March 2010, resulted in an early lakewide ice-free

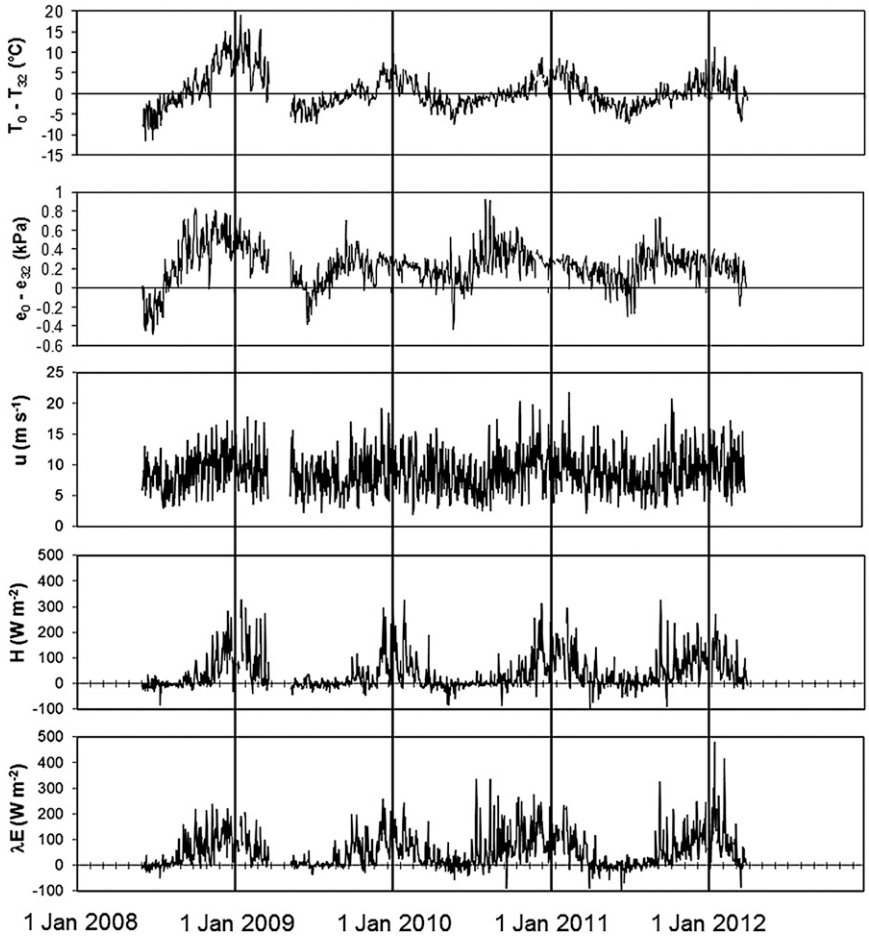

FIG. 2. Daily, 24-h-mean time series of (top to bottom) temperature and vapor pressure gradients, wind speed, and turbulent fluxes observed at Stannard Rock over the 4-yr study period.

date of 9 April (Table 1). This ice breakup, four weeks ahead of the previous year, provided the opportunity for 500 MJ m^{-2} more energy to be stored in the water column during the spring of 2010, as compared to 2009. This extra energy had several effects. First, it resulted in a warm T_0 of 8.5°C on 1 June 2010. Second, the relatively warm lake and positive vapor pressure gradients meant relatively more net radiation (29%) could be directed to turbulent fluxes during the summer months (Table 1). June through August cumulative evaporation was 70 mm in 2010 versus 15 and 21 mm in 2008 and 2009, respectively (Fig. 4, Table 2). Evaporation rates during the winter of 2010/11 (3.2 mm day^{-1}) were also ~30% higher than the previous two winters (2.5 mm day^{-1}) because of stronger winds and vapor pressure gradients. The longer evaporation year (393 days) and higher average daily evaporation rates (1.9 mm day^{-1}) in 2010/11 resulted in the highest annual evaporation loss of the 4-yr study period (749 mm; Table 2, Fig. 4).

d. Evaporation year 2011/12

Similar to 2010, net radiation during the spring of 2011 became positive over the lake surface five weeks earlier than in 2009. For both years, however, this was not simply because of a lack of ice, because decreases in reflected shortwave radiation with changes in albedo were offset by increases in outgoing longwave radiation with warmer surface temperatures (Fig. 5). As such, the increased net radiation was primarily due to higher incoming shortwave radiation (perhaps because of a decrease in cloud cover). Consistent advection of cold air in March 2011 kept the mean T_{32} near −2.5°C with only 10 thawing degree-days, which was cooler than conditions in March 2009 when there was extensive ice cover. These spring atmospheric conditions allowed the lake to stay cold, such that T_0 on 1 June 2011 was 3°C lower than 2010, despite comparable antecedent ice conditions. Net radiation was directed almost entirely to lake heat storage during the summer of

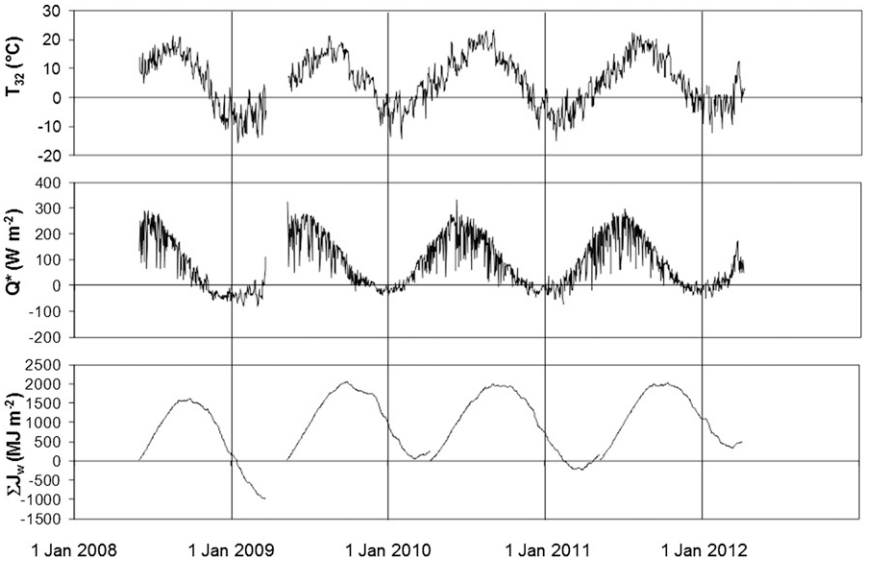

FIG. 3. Daily, 24-h-mean time series of T_{32}, Q^*, and J_w observed at Stannard Rock over the 4-yr study period. In the figure lake heat storage is reset to zero at the beginning of each evaporation year to aid comparison among years.

2011, rather than turbulent fluxes. Negative vapor pressure gradients led to condensation through the summer for the first time in the study period. This was followed by a warm November, with an average T_{32} of 4°C and 7 FDD. The maximum ice-covered fraction (F_{Imax}) during the winter of 2011/12 and seasonally averaged ice covered fraction (F_{Imean}) across the lake only reached 0.10 and 0.03, respectively, which was the lowest of the study period (Table 1). Average winter evaporations rates (3.6 mm day^{-1}) were the highest of the study period, associated with strong vapor pressure gradients and high winds, thereby offsetting the delayed start to the evaporation season. Total water lost to evaporation through the 331-day-long 2011/12 evaporation year was 574 mm (Table 2, Fig. 4), which was ~8% higher than 2008/09 and 2009/10 and ~23% less than 2010/11.

4. Discussion

a. The shoulder seasons: Spring and autumn

This study highlights the importance of the ''shoulder seasons'' (i.e., spring and autumn) to the evaporation regime of Lake Superior. Subtle changes in the distribution of air temperature in November and March profoundly shape antecedent conditions that affect evaporation for several subsequent cold and warm months, respectively. Conditions in November 2008 and 2010 provide two contrasting cases (Fig. 6). Surface water temperatures averaged around 10°C in October of both years, but air temperatures in the subsequent month of November had very different distributions, with 12 fewer freezing degree-days in 2010 (Table 1). The difference in freezing degree-days and average monthly air temperature between the two years was due simply to the passage of one particularly cold low pressure system during 16–22 November 2008. This low was just east of Lake Superior on 20 November 2008 and, in combination with a low to the north, brought in cold air (−4.5°C) and high winds (16 m s^{-1}), creating a highly unstable surface ($\zeta = -2.4$; a dimensionless stability parameter calculated as z/L, where z is the measurement height and L is the Obukhov stability length). This one event provided 17 freezing degree-days. Sensible and latent heat fluxes during

TABLE 1. A variety of key indicators of the Lake Superior evaporation regime. TDD is thawing degree-days.

Evaporation year	2008/09	2009/10	2010/11	2011/12
Preceding March T_{32} (°C)	−2.2	−3.2	2.1	−2.5
Preceding March TDD	3	35	79	10
Ice-free date	14 May 2008	7 May 2009	9 Apr 2010	7 May 2011
Date $Q^* > 0$	n/a	15 Mar 2009	9 Feb 2010	7 Feb 2011
1 June T_0 (°C)	6.3	2.7	8.5	5.0
Jun–Aug J_w/Q^*	1.0	0.95	0.71	1.0
Nov T_{32} (°C)	2.2	5.5	3.4	3.9
Nov FDD	29	1	17	7
F_{Imax} (lake)	0.95	0.28	0.31	0.10
F_{Imax} (footprint)	0.95	0	0	0
F_{Imean} (lake)	0.32	0.05	0.09	0.03
F_{Imean} (footprint)	0.35	0	0	0

TABLE 2. Monthly average daily evaporation rates and seasonal and evaporation year totals. Summer is June–August. Winter is defined as 1 November through to breakup. A blank month was not part of the evaporation year, and n/a denotes that data were unavailable; ΣE is cumulative evaporation.

Monthly mean evaporation (mm day^{-1})	2008/09	2009/10	2010/11	2011/12
April			0.6	
May	n/a	0.2	0.08	−0.1
June	−0.1	0.1	0.4	−0.1
July	0.05	0.05	0.07	0.0
August	0.5	0.5	1.9	0.2
September	2.0	1.1	2.9	1.9
October	2.9	2.3	3.6	1.4
November	2.8	1.5	3.4	2.6
December	3.5	4.2	4.2	4.0
January	2.2	3.6	3.1	4.2
February	1.8	2.6	3.2	3.6
March	1.1	0.8	1.6	1.2
April	0.4	0.8	−0.2	0.1
May	0.2		−0.7	
Seasonal and annual values				
Summer ΣE (mm)	15	21	70	5
Winter ΣE (mm)	354	395	467	471
Evaporation year ΣE (mm)	520	525	749	574
Length of evaporation year (days)	358	337	393	331
Evaporation year daily average (mm day^{-1})	1.5	1.6	1.9	1.7

the passage of this event averaged 128 and 139 W m^{-2}, respectively. Evaporation peaked at 7.5 mm day^{-1} on 20 November 2008. Overall, the lake lost 185 MJ m^{-2} of heat during the week, almost half the monthly total.

In terms of monthly mean air temperatures, there was only a small difference (~1.2°C) in 2008 and 2010 mean November T_{32}, yet the eventual maximum ice coverage in 2008 was roughly 3 times that of 2010 (Table 1). Clearly, the factors for creating extensive ice conditions include both antecedent water temperatures at the start of the fall/winter seasons, as well as the total heat loss experienced by the lake during this period of rapid cooling. Lake Superior surface water temperatures average around 7° ± 1°C in November, and with such little variation, antecedent water temperatures in late fall are not likely to account for much of the interannual variability in ice conditions. Support for this is provided by a comparison of conditions during 2008 and 2009. Surface water temperatures were near normal in 2008, and the lake would have required approximately 400 MJ m^{-2} of heat loss to cool the upper 10 m of the water column to the freezing mark. As it turned out, conditions in November 2008 enabled roughly 98% of this required heat loss. The passage of the cold front in November 2008 provided a large proportion of the required cooling that winter (45%) via 17 freezing degree-days, and in only one week's time. In contrast, November 2009 surface water temperatures were slightly colder (5°C), but the one freezing degree-day and 107 MJ m^{-2} heat loss experienced by the lake provided only 36% of the heat loss required to cool the upper 10 m of the water column to 0°C.

Thus, the particularly strong cold front in 2008 put mean November air temperatures on the cold side of a ''threshold'' that appears to form near 27 FDD (Fig. 7), below which lower-than-normal ice cover fractions tend to occur. This implies that by shaping the average and

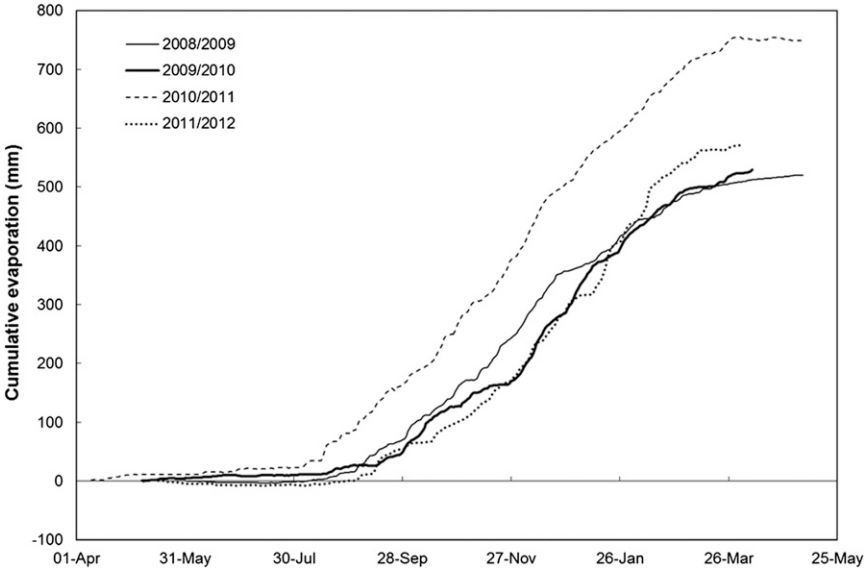

FIG. 4. Cumulative evaporation for each evaporation year for the period of study.

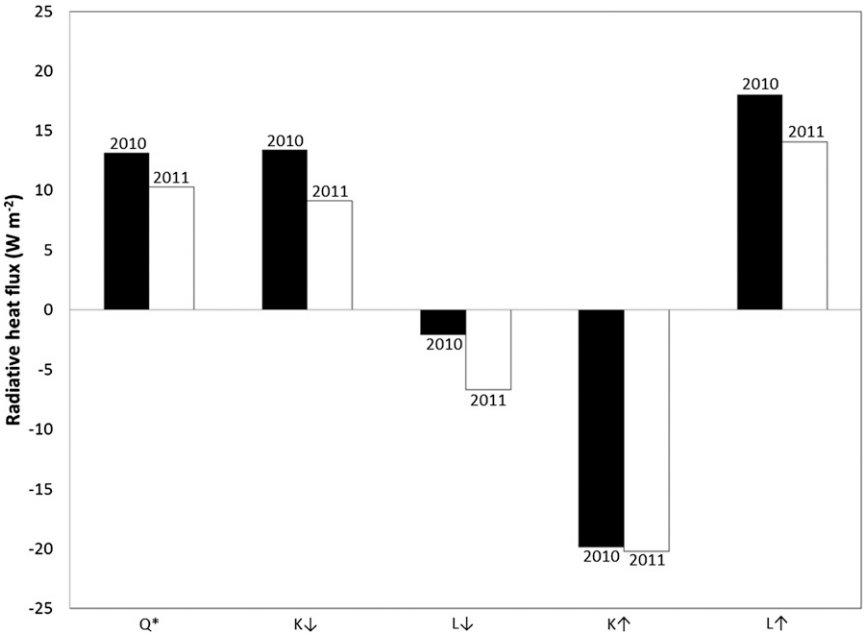

FIG. 5. Difference in surface radiative heat flux during February 2010 and 2011 (ice absent from footprint) as compared to February 2009 (ice present in footprint).

distribution of air temperatures, single synoptic-scale events can generate disproportionately large heat loss and strongly influence whether or not the lake cools enough to form expansive ice cover. As the discussion above implies, this may influence evaporation rates for several subsequent months. There are a few instances when a colder-than-normal November was followed by anomalously low ice cover later that winter (Fig. 7), but the general pattern shows that most of the low-ice winters are preceded by warmer-than-normal Novembers. Furthermore, the relationship in Fig. 7 is statistically significant at the 95% level (r^2 = 0.32; Table 3). November is not the month with the strongest relationship between FDD and F_{Imean}. January and February exhibit even stronger relationships with ice extent with r^2 of 0.35 and 0.40, respectively (Table 3). However, given the comparable regression values across the three months and far fewer freezing degree-days in November (Fig. 6), it could be argued that the ''efficiency'' of a freezing degree-day in November in leading to high ice cover is greater than that in January or February. It is interesting to note that while FDD in other

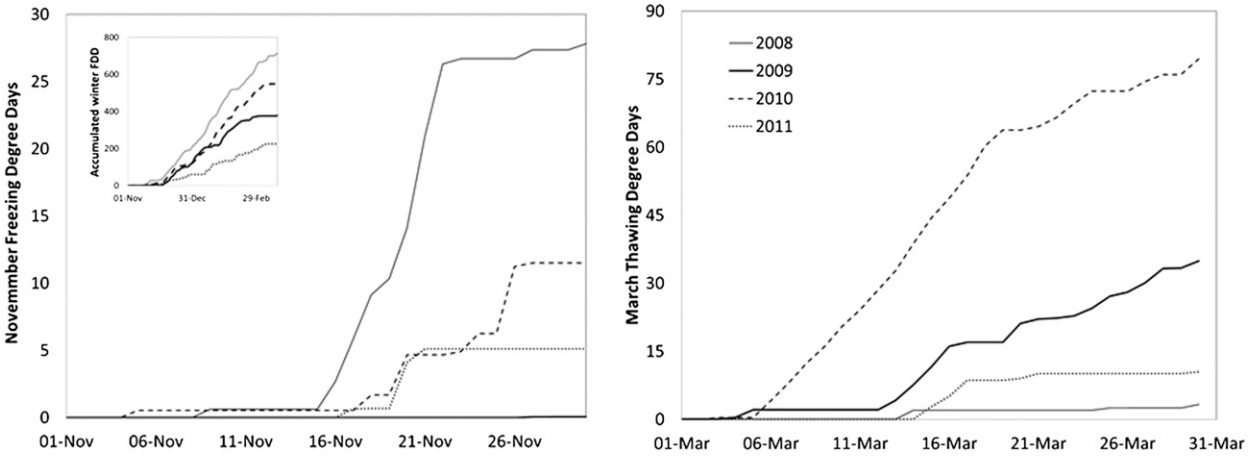

FIG. 6. (left) November FDD and (right) March thawing degree-days for the period of study. The inset is the accumulated FDD for the period of study, to put into the context November conditions relative to the rest of the winter.

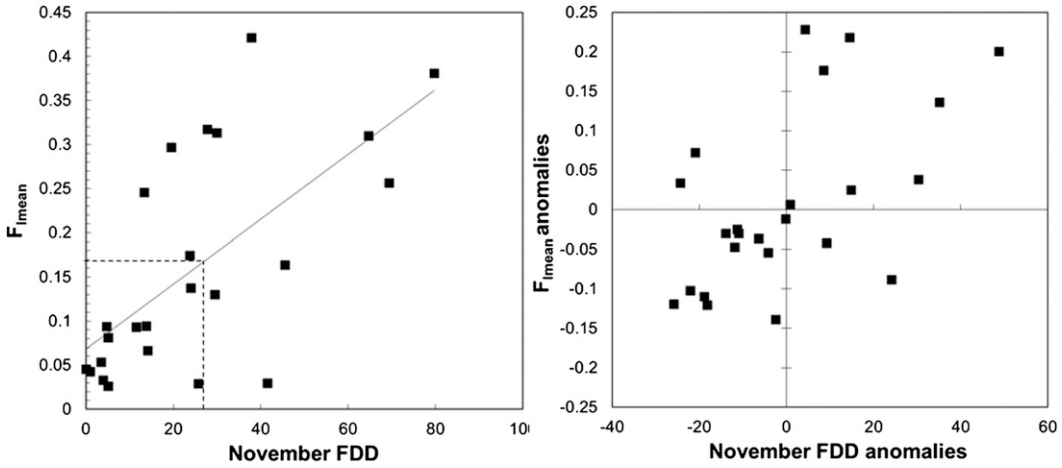

FIG. 7. (left) November FDD from the NOAA NDBC STDM4 period of record (1984–2012) vs seasonally averaged fraction of ice cover across Lake Superior, as measured by the Canadian Ice Service. The horizontal dashed line at 0.17 represents the mean value of F_{Imean} and the vertical line descends to a threshold of 27 November FDD above which higher-than-average ice cover tends to form. (right) Detrended anomalies of the same November FDD and seasonally averaged fraction of ice cover values.

winter months have no significant linear trend over time, a decreasing trend in November to below the 27 FDD threshold is clearly evident (Fig. 8). This warming trend is also evident in the mean and maximum Lake Superior ice concentrations (Fig. 8), both of which show a shift in regime around 1998 to lower values. This suggests that the observed trends toward less ice cover on Lake Superior (Wang et al. 2012) are strongly related to changes in atmospheric conditions during November.

Similar to autumn, climatic conditions during the spring shoulder season can also play an important role in subsequent Lake Superior water temperatures and evaporation rates. For example, the advection of warm air over Lake Superior in March 2010 resulted in a very different distribution of March thawing degree-days than in the other study years (Fig. 6). There may be a similar threshold in March thawing degree-days or average air temperatures that is indicative of the ice-free date and, in turn, surface water temperatures at the beginning of the summer. The results shown in Table 1 suggest that this threshold may be at (or just below) the freezing mark, but the wide disparity between the March T_{32} in 2010 and the other study years prevents a definitive identification of this value, if it even exists. Clearly, a longer-term study of March temperatures and Lake Superior ice-off dates is required to answer this question. It would appear, however, that if T_0 is above ~7°C on 1 June at offshore locations such as around Stannard Rock, then Lake Superior is likely to be warm enough to allow for earlier and enhanced latent heat fluxes during the summer period (Table 1). The 2010/11 evaporation year is a good example of how much this scenario can lead to a significant enhancement of total evaporative water loss.

b. The role of ice

Taking into account the range of uncertainty in the evaporation measurements (10%–20%), it is notable that for two of the study years—one with high F_{Imax} (2008/09; 95%) and the other with low F_{Imax} (2009/10; 0%)—cumulative winter and annual evaporation were essentially indistinguishable (Tables 1 and 2). This is primarily because the high heat storage losses in November that are required to form extensive ice cover are also accompanied by very high evaporation losses. These are then partially offset by lower evaporation rates once ice cover forms, but only after the ice-covered fraction within the footprint exceeds 0.5, which typically does not occur until mid-March. March evaporation rates in all of the four years were generally low, as air temperature is increasing at this time of year and gradients change sign from positive to

TABLE 3. Explanation of variance (i.e., r^2 value) between FDD in winter months and time, F_{Imax}, and F_{Imean}. Detrended anomalies of F_{Imax} and F_{Imean} were analyzed to remove any influence of cross correlation with time. Significant relationships (at the 95% level) are in bold.

Month	r^2 vs year	r^2 vs F_{Imax}	r^2 vs F_{Imean}
November	**0.18**	**0.25**	**0.32**
December	0.02	**0.18**	0.15
January	0.004	**0.25**	**0.35**
February	0.07	**0.35**	**0.4**
March	0.13	0.16	**0.22**

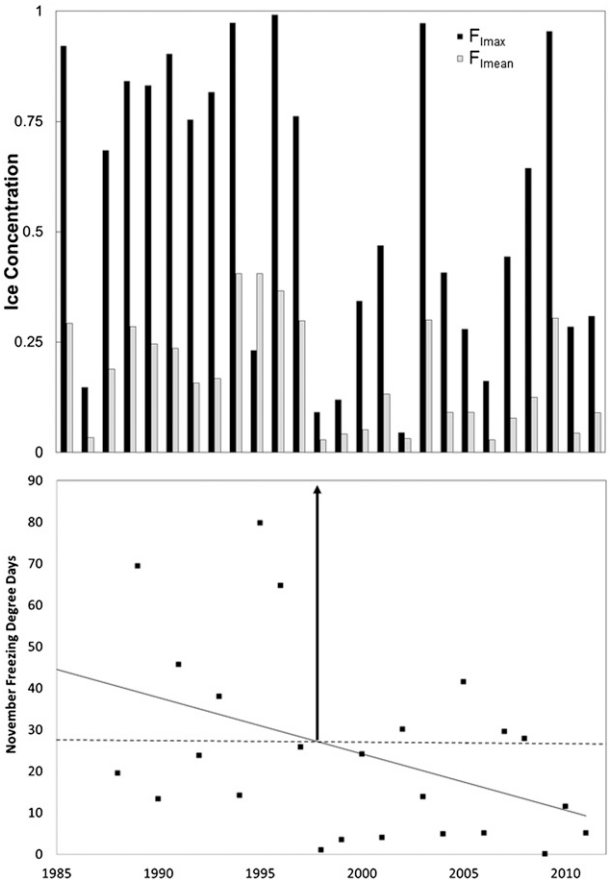

FIG. 8. (top) Lake Superior F_{Imax} and F_{Imean} for the period of record from the Canadian Ice Service (1986–2012) and (bottom) November FDD for the period of record from NOAA NDBC STDM4 (1984–2012) vs time. The best fit line between FDD and time is shown, as is a horizontal line denoting the 26 November FDD threshold between above-average and below-average seasonally averaged ice fraction, the intersection of which occurs in 1998.

negative (Figs. 2, 3; Table 2). Furthermore, March evaporation rates were actually higher during the heavy-ice year of 2008/09 than the low-ice year of 2009/10 because of anomalously warm conditions and weak vapor pressure gradients. Because extensive ice cover comes so late in the evaporation season, the window of opportunity to suppress total evaporation during heavy-ice years is too short to more than offset the enhanced evaporation from the preceding fall and early winter. That said, the effects of ice can be delayed until the next evaporation year, as occurred in 2010/11, when early ice breakup and warm summer water temperatures led to an early start to the evaporation season. This pattern is consistent with the results of Blanken et al. (2011), who defined ''annual'' as the water year (1 October to 30 September). Blanken et al. (2011) presented data that showed a 28% lower total evaporation in the high-ice 2008/09 water year (464 mm) versus the low-ice 2009/10 water year (645 mm), which partially overlap the 2009/10 (525 mm) and 2010/11 (749 mm) ''evaporation years'' defined here using the ice-free date. Therefore, it is an important conclusion that a high fractional ice cover does not necessarily immediately translate into low winter evaporation totals during the same winter. Rather, the more profound impacts of ice cover reduction can be delayed for several months into the subsequent evaporation season. Furthermore, the definition of ''year'' or ''annual'' varies in the literature according to calendar, water, or evaporation years, indicating that careful consideration is needed when evaluating and comparing the results from different studies.

On large northern lakes, it is not just the maximum ice cover extent that is important, but also the duration and timing of ice cover (Blanken et al. 2000). An earlier breakup and subsequent lack of ice in April and early May leads to higher water surface temperatures in summer, since energy during this period of increasing incident solar radiation input can be directed toward heating the water, rather than melting ice or being reflected. This is followed by a subsequent earlier start to the next evaporation season and enhanced summer evaporation, which is typified by the summer of 2010. The summer of 2011, on the other hand, was characterized by low water temperatures and suppressed evaporation rates because of cool atmospheric conditions. This delay in the beginning of the evaporation year occurred *despite* low ice extents during winter 2010/11 that were very similar to 2009/10. In fact, the last three winters in this study all experienced very low values of F_{Imax} and F_{Imean} (~10%–30% and 3%–9%, respectively, lakewide; 0% within the footprint), yet they also exhibited very different winter, summer, and annual evaporation losses. Furthermore, these evaporation totals were sometimes even indistinguishable from the one year with high F_{Imax} (2008/09). Thus, low ice extent does not necessarily result in enhanced evaporation that winter, or even higher yearly totals. Rather, it requires a combination of low ice extent, higher March air temperatures, and an early ice breakup to lead to an early start to the summer evaporation season and, subsequently, high annual evaporation totals (such as in 2010/11; Tables 1 and 2). This is not the sole condition for enhanced evaporation, and there are feedbacks between sensible heat transfer, air temperatures, vapor pressure gradients, and evaporation that could be better defined. However, this documented pattern aligns with previous long-term studies that show that as the climate has warmed, the attendant increases in Lake Superior evaporation have been most evident in the summer months rather than winter (Lenters 2004; Hanrahan et al. 2010). It is also consistent with the findings of Austin and Colman (2007),

while at the same time suggesting that it is not just declining ice cover extent on Lake Superior that is important to increasing summer water temperatures, but also the timing of breakup.

c. *Short- and long-term prediction*

Society has little direct control over severe lake level decline caused by high evaporation, but rather can only adapt to and mitigate such changes. Accurate hydrometeorological prediction is of paramount importance for making sound water resource management decisions in this context. Current 6-month forecasts of Great Lakes water levels are probabilistic and therefore use previous records. However, it is becoming abundantly clear that the Laurentian Great Lakes climate is not stationary (Austin and Colman 2007; Stow et al. 2008). This has led some to apply more physically based numerical prediction models for short-term forecasts (Gronewold et al. 2011), as well as large-scale climate models to long-term prediction (Angel and Kunkel 2010), although the merits of methodologies in the latter have been questioned by others (Kundzewicz and Stakhiv 2010). The high degree of persistence with which air temperatures influence the Lake Superior evaporation regime is epitomized by the impact of individual synoptic systems in November 2008 and March 2010. Furthermore, these systems are not driven by local conditions over Lake Superior, but by large-scale regional atmospheric flow. If the aforementioned models are to be used effectively for water resource supply prediction, they need to demonstrate an ability to accurately represent the strong coupling between synoptic-scale atmospheric flow, Lake Superior ice, temperature, and interannual variations in evaporation and overall evaporation regimes. This includes encapsulating the effects that single, synoptic-scale events can have on lake thermal conditions that further influence evaporation for several months, if not a full year.

5. Concluding remarks

During this particular 4-yr study period, ice cover extent was not found to be a simple predictor of Lake Superior evaporation. There is a slight tendency for less ice coverage to be associated with enhanced winter evaporation rates, but the connection with annual evaporation totals is much more complex and often contrary to what might be expected. This results from the fact that a low-ice winter generally requires reduced surface heat fluxes during the preceding autumn (i.e., low evaporation rates). On the other hand, a low-ice scenario combined with an early breakup permits more energy to be absorbed by the lake, which will lead to a longer and enhanced evaporation season the subsequent summer and autumn. Thus, the interaction between Lake Superior evaporation and ice cover is, to a large degree, compensatory, once the full seasonal cycle is taken into account.

The annual evaporation regime of Lake Superior is found to be strongly dependent on synoptic events during the spring and autumn, typified by conditions in November and March. The physical processes important to Lake Superior evaporation patterns include absorption of solar radiation in the spring and turbulent flux processes in the autumn. Specifically, conditions in November exert a strong control on whether the lake loses enough heat to enhance evaporation early in winter and form an extensive ice cover. Higher or lower air temperatures in November weaken or strengthen temperature and humidity gradients, suppressing or enhancing latent heat fluxes and lake heat storage losses, respectively. Synoptic-scale events of only 4–7 days in length during November are capable of bringing in enough cold air over the lake to increase freezing degree-days above thresholds that significantly contribute to widespread ice cover. Conversely, if these events do not occur, there is a higher likelihood of the absence of ice across the lake. Either situation profoundly shapes antecedent lake thermal conditions that then dictate evaporation for several subsequent months. Air temperatures in March influence the timing of ice breakup, which in turn dictates the amount of energy absorbed by the lake, surface water temperatures the following summer, and corresponding evaporation rates.

The results presented in this 4-yr, enhanced observation campaign imply that air temperature at key times of the year (i.e., November and March) is a major factor that defines the Lake Superior evaporation regime and interannual variability via ice cover and lake heat budget processes. An increasing trend in November air temperatures has led to reductions in ice cover on Lake Superior, with impacts on the evaporation regime. The area around Stannard Rock is admittedly a small portion of the lake, but measurements there have proven to be representative of lakewide response, and the period studied here includes the range of ice conditions that can occur at Stannard Rock and across the lake. To conclusively clarify the interactions among ice cover, water temperature, and evaporation and show the effect on the regime of the entire lake, analysis of long-term, spatially distributed model output is needed. In doing so, it is essential that regional climate and numerical weather prediction models properly represent synoptic-scale processes that influence long-term evaporation regimes through lake heat storage–ice–evaporation feedbacks. Sound models are becoming increasingly important as water resource specialists advocate for adaptive management of Lake

Superior water levels. Adaptive management is easier when tools can predict lake levels across a range of time scales and properly identify the cause of water level trends with a minimum of uncertainty. Demonstrating a robust ability to capture the mechanisms by which short events can create conditions with long-term persistent effects would reduce uncertainty and provide confidence that these models can act the foundation for providing data and information crucial for adaptive management.

Acknowledgments. Funding for this research was provided by the International Joint Commission through the International Upper Great Lakes Study, as well as the Great Lakes Integrated Sciences and Assessments (GLISA) Center. The authors wish to thank the Kimar family of Au Train, Michigan, for their logistical assistance and hospitality and Jeff Gamble of the Big Bay Lighthouse for assisting in the remote collection of field data. The United States Coast Guard provides access to the Stannard Rock Light. We thank the editor and three anonymous reviewers who provided constructive comments for improving the manuscript.

REFERENCES

Angel, J. R., and K. E. Kunkel, 2010: The response of Great Lakes water levels to future climate scenarios with an emphasis on Lake Michigan-Huron. *J. Great Lakes Res.,* **36,** 51–58.

Assel, R. A., F. H. Quinn, and C. E. Sellinger, 2004: Hydroclimatic factors of the recent recod drop in Laurentian Great Lakes water levels. *Bull. Amer. Meteor. Soc.,* **85,** 1143–1146.

Austin, J. A., and S. M. Colman, 2007: Lake Superior summer water temperatures are increasing more rapidly than regional air temperatures: A positive ice-albedo feedback. *Geophys. Res. Lett.,* **34,** L06604, doi:10.1029/2006GL029021.

Baldocchi, D. D., B. B. Hicks, and T. P. Meyers, 1988: Measuring biosphere–atmosphere exchanges of biologically related gases with micrometeorological methods. *Ecology,* **69,** 1331–1340.

Beletsky, D., J. H. Saylor, and D. J. Schwab, 1999: Mean circulation in the Great Lakes. *J. Great Lakes Res.,* **25,** 78–93.

Blanken, P. D., and Coauthors, 2000: Eddy covariance measurements of evaporation from Great Slave Lake, Northwest Territories, Canada. *Water Resour. Res.,* **36,** 1069–1077.

——, C. Spence, N. Hedstrom, and J. D. Lenters, 2011: Evaporation from Lake Superior: 1. Physical controls and processes. *J. Great Lakes Res.,* **37,** 707–716.

Croley, T. E., and R. A. Assel, 2002: Great Lakes evaporation model sensitivities and errors. Proc. Second Federal Interagency Hydrologic Modeling Conference. Las Vegas, NV, Subcommittee on Hydrology of the Interagency Advisory Committee on Water Data, 12 pp. [Available online at http://www.glerl.noaa.gov/pubs/fulltext/2002/20020004.pdf.]

Derecki, J. A., 1981: Operational estimates of Lake Superior evaporation based on IFYGL findings. *Water Resour. Res.,* **17,** 1453–1462.

Desai, A. R., J. A. Austin, V. Bennington, and G. A. McKinley, 2009: Stronger winds over a large lake in response to weakening air-to-lake temperature gradient. *Nat. Geosci.,* **2,** 855–858.

Gerbush, M. R., D. A. R. Kristovich, and N. F. Laird, 2008: Mesoscale boundary layer and heat flux variations over pack ice–covered Lake Erie. *J. Appl. Meteor. Climatol.,* **47,** 668–682.

Gronewold, A. D., A. H. Clites, T. S. Hunter, and C. A. Stow, 2011: An appraisal of the Great Lakes advanced hydrologic prediction system. *J. Great Lakes Res.,* **37,** 577–583.

Hanrahan, J. L., S. V. Kravtsov, and P. J. Roebber, 2010: Connecting past and present climate variability to the water levels of Lakes Michigan and Huron. *Geophys. Res. Lett.,* **37,** L01701, doi:10.1029/2009GL041707.

Horst, T. W., 1997: A simple formula for attenuation of eddy fluxes measured with first order response scalar sensors. *Bound.-Layer Meteor.,* **94,** 517–520.

Kundzewicz, Z. W., and E. Z. Stakhiv, 2010: Are climate models ''ready for prime time'' in water resources management applications, or is more research needed? *Hydrol. Sci. J.,* **55,** 1085–1089.

Laird, N. F., and D. A. R. Kristovich, 2002: Variations of sensible and latent heat fluxes from a Great Lakes buoy and associated synoptic weather patterns. *J. Hydrometeor.,* **3,** 3–12.

Lenters, J. D., 2004: Trends in Lake Superior water budget since 1948: A weakening seasonal cycle. *J. Great Lakes Res.,* **30,** 20–40.

Lofgren, B. M., and Y. Zhu, 2000: Surface energy fluxes on the Great Lakes based on satellite observed surface temperatures 1992 to 1995. *J. Great Lakes Res.,* **26,** 305–314.

Massman, W. J., 2000: A simple method for estimating frequency response corrections for eddy covariance systems. *Agric. For. Meteor.,* **104,** 185–198.

Mishra, V., K. A. Cherkauer, and L. C. Bowling, 2011: Changing thermal feedbacks in the Great Lakes region: Role of ice cover feedbacks. *Global Planet. Change,* **75,** 155–172.

Morton, F. I., 1967: Evaporation from large deep lakes. *Water Resour. Res.,* **3,** 181–200.

Neff, B. P., and J. R. Nicholas, 2005: Uncertainty in the Great Lakes water balance. USGS Scientific Investigations Rep. 2004-5100, 42 pp. [Available online at http://pubs.usgs.gov/sir/2004/5100/pdf/SIR2004-5100.pdf.]

Schertzer, W. M., 1978: Energy budget and monthly evaporation estimates for Lake Superior, 1973. *J. Great Lakes Res.,* **4,** 320–330.

Schuepp, P. H., M. Y. LeClerc, J. L. MacPherson, and R. L. Desjardines, 1990: Footprint prediction of scalar fluxes from analytical solutions of the diffusion equation. *Bound.-Layer Meteor.,* **36,** 355–373.

Spence, C., P. D. Blanken, N. Hedstrom, V. Fortin, and H. Wilson, 2011: Evaporation from Lake Superior: 2. Spatial distribution and variability. *J. Great Lakes Res.,* **37,** 717–724.

Stow, C. A., E. C. Lamon, T. K. Kratz, and C. E. Sellinger, 2008: Lake level coherence supports common driver. *Eos, Trans. Amer. Geophys. Union,* **89,** 389–390.

Tanny, J., S. Cohen, S. Assouline, F. Lange, A. Grava, D. Berger, B. Teltch, and M. B. Parlange, 2007: Evaporation from a small water reservoir: Direct measurements and estimates. *J. Hydrol.,* **351,** 218–229.

Wang, J., X. Bai, G. Leshkevich, M. Colton, A. Clites, and B. Lofgren, 2010: Severe ice cover on Great Lakes during winter 2008–2009. *Eos, Trans. Amer. Geophys. Union,* **91,** 41–42.

——, ——, H. Hu, A. Clites, M. Colton, and B. Lofgren, 2012: Temporal and spatial variability of Great Lakes ice cover, 1973–2010. *J. Climate,* **25,** 1318–1329.

Webb, E. K., G. I. Pearman, and R. Leuning, 1980: Correction of flux measurements for density effects due to heat and water vapour transfer. *Quart. J. Roy. Meteor. Soc.,* **106,** 85–100.